IEEE Access
Multidisciplinary | Rapid Review | Open Access Journal

Received July 30, 2018, accepted September 6, 2018, date of publication September 17, 2018, date of current version October 8, 2018.

Digital Object Identifier 10.1109/ACCESS.2018.2870292

Robust-Adaptive Controller Design for Robot Manipulators using the $\mathcal{H}_\infty$ Approach

RAMEEZ HAYAT[1,2], MARION LEIBOLD[1], AND MARTIN BUSS[1,2]
[1]Chair of Automatic Control Engineering, Technical University of Munich, 80333 Munich, Germany
[2]TUM Institute for Advanced Study, Technical University of Munich, 85748 Garching, Germany

Corresponding author: Rameez Hayat (rameez.hayat@tum.de)

This work was supported in part by the German Research Foundation, in part by the Technical University of Munich through the Framework of the Open Access Publishing Program, and in part by the Higher Education Commission of Pakistan through the Faculty Development Program UESTP.

ABSTRACT This paper proposes a model-free robust-adaptive controller for Euler–Lagrange systems with a quantitative performance analysis in terms of state-errors. The controller has only few parameters, and the procedure of finding the controller parameters is intuitive and easy to implement. The controller acts as an adaptive computed-torque controller and consists of two feedback loops: the inner loop evaluates the robot dynamics to linearize the system and the outer loop is a simple proportional derivative controller. Input-to-state stability is used to derive the control law and tune the controller parameters. Inverse-optimal control using the Hamilton–Jacobi–Isaacs equations is utilized to confirm the optimality of the controller. Robustness of the proposed controller is proved using the $\mathcal{H}_\infty$ optimality technique. The controller starts with zero system information and adapts itself to the real system dynamics. Finally, the proposed technique is validated on a three-degree-of-freedom and a seven-degree-of-freedom robot manipulator.

INDEX TERMS Adaptive control, $\mathcal{H}_\infty$ optimal control, Hamilton-Jacobi-Isaacs, input-to-state-stability, computed torque, Euler-Lagrange.

I. INTRODUCTION

After many decades of research, the controller design for a robot manipulator is still a contemporary field of research [1]–[5]. The difficulty associated with robot controllers is due to the complexity of the robot dynamics and the strong coupling between the joints [6], [7]. A well-known state-of-the-art controller design technique applies feedback linearization, also known as computed torque method [8], [9]. By using such a controller, a simple proportional-derivative (PD) controller can be utilized to achieve desired tracking performance. However, computed-torque controllers are model-based controllers and their performance depends on the estimated system parameters.

Thus high performance is often not achieved using a computed-torque technique due to un-modeled system dynamics, disturbances and parameter uncertainties. For instance, only linear friction models are used in many controller designs [10], [11], and thus many traits of friction are ignored such as Coulomb's and static friction. Further, torque saturation and variation in the actuator gains usually deteriorate the performance. There are many reasons for parameter uncertainties, e.g., lumped parameter models or the effect of temperature variation on friction. Different types of control methods have been introduced to overcome the above mentioned issues, such as robust control [5], [12]–[14], adaptive control [2], [3], [15], neural network control [16], [17], observer-based control [18], [19], orbital stabilization based control [20] and sliding mode control [21], [22].

The dynamics of a robot is given by the Euler-Lagrange equations. If uncertainties in the system dynamics appear only in the constant coefficients, e.g. masses or lengths of joints, we can reformulate the Euler-Lagrange equations into a state-dependent regressor matrix and an unknown constant coefficient vector. Many of the existing adaptive controllers are Lyapunov-based [23]–[29] and take advantage of this fact, and Lyapunov's descent property is then used to find the unknown coefficient vector [23]. Calculation of the regressor matrix, especially for a high degree-of-freedom (DoF) manipulator, is a complicated task if there are many system parameters. The function approximation technique (FAT) approximates the system dynamics by linear orthogonal basis functions [2], [3] to avoid the evaluation of the regressor matrix. For Lyapunov-based controllers, tuning of the controller parameters and implementation on a higher DoF manipulator

is difficult and requires trial and error to achieve acceptable performance. These controllers are theoretically sound; however, practical implementations are difficult because they focus more on stability and less on performance. Another class of controllers are sliding mode controllers [22], [30]. Sliding mode controllers have the advantage that they are simple, robust and usually model-free. A major problem in sliding mode controllers is chattering. Next, we discuss some model-free control methods. Zhang and Yan [31] proposed a multi-dimensional Taylor network inverse-control method that has a low computational complexity. Fateh *et al.* [32] proposed a controller based on a discrete fuzzy estimator. In [33], an adaptive control method is presented that consists of two robust adaptive laws for the estimation of the system. The Lyapunov stability theorem is then used to ensure the stability of the system.

The controllers discussed so far lack a quantitative performance analysis, and there is no optimality mentioned in these techniques [34]. Therefore next, we discuss techniques that provide a performance analysis. A model-free robust control method is proposed in [35] that ensures a prescribed transient and steady-state performance. The controller uses stable linear filters that force the states to satisfy the desired performance, however, the controller does not give optimal result and it is only tested on a 2-DoF robot manipulator. Orbital-stability based controller design [20] uses the transverse dynamics to control a manipulator. The controller makes sure that the states of the system remain in an orbit around the desired trajectory. This is useful for under-actuated system, but the controller requires knowledge of the system model for implementation, and there is no discussion on how to deal with model mismatch or external disturbances. Another approach is the $\mathcal{H}_\infty$ optimality, which has been recently used to enable a quantitative performance analysis and robustness against disturbances [12], [36]. The major obstacle in this technique is the need of finding an analytical solution of the Hamilton-Jacobi-Isaacs (HJI) equation. Fortunately, for Euler-Lagrange equations, the solution of the HJI equations was shown to exist [13], [37]. Choi *et al.* [12] proposed an inverse-optimal proportional-integral-derivative (PID) controller that is based on the $\mathcal{H}_\infty$ technique. The controller is relatively easy to implement while giving optimal performance, but an estimate of the system parameters is required to find the controller parameters. We will show that a specific case of the controller introduced in this paper is similar to this robust controller because both act like a PID controller. However, the performance criteria are different, and it will be easier and more intuitive to find the controller parameters for the adaptive controller proposed here.

This paper introduces a model-free robust-adaptive controller design method that sustains a predefined performance. The performance is guaranteed by keeping the steady-state joint-error smaller than a threshold value. Like an inverse-dynamical controller, the proposed controller has two feedback loops: the inner loop is adaptive and estimates the system dynamics for cancellation of the non-linearities and the outer loop is a PD controller. A simple linear differential equation is formulated to evaluate the adaptive part. An advantage of the proposed controller is that it neither requires an estimated system model nor a regressor matrix and acts like a model-free adaptive controller. Moreover, the controller only uses the joint velocities, joint angles and integrals of joint angles to calculate the control input.

The controller design considers two aspects: first, an $\mathcal{H}_\infty$ approach is used to ensure the robustness and a prescribed performance. Second, the adaptation of the estimated system dynamics towards the real dynamics is ensured without any initial knowledge about the real system. We represent the robotic system as an $\mathcal{L}_2$-gain system and using HJI equations, we prove that the controller is robust. We use an inverse-optimal control method to find the matrices for the HJI equations, i.e., "given a controller, evaluation of the $\mathcal{L}_2$-gain that satisfies the robustness". Thus, we get a simple controller with only few controller parameters. The effect of external disturbances is significantly reduced using input-to-state stability (ISS). It is also the tool used in this article to derive a general form of the adaptive controller. Another advantage of using ISS is that the parameters of the controller can be determined depending on desired performance specifications. The estimation of system dynamics is important because it is then used to linearize the overall feedback system, thus winding up as an adaptive computed-torque method.

In summary, the state-of-the-art robust/adaptive controllers have one or more of the following limitations: no optimality, high computational cost, dependence on system parameters, no quantitative performance analysis and challenging tuning of the control parameters. This paper addresses the issues mentioned above apart from stability, robustness and straightforward implementation. However, the primary focus is the performance and relatively simple implementation of the controller, especially for high DoF manipulators. The performance of the proposed controller is validated by experiments using a 3-DoF and a 7-DoF robotic manipulator.

The remainder of the paper is organized as follows: the main contribution of the paper, which is a novel robust-adaptive controller, is summarized in Sec. II. The robustness shown by the $\mathcal{H}_\infty$ inverse-optimal control is discussed in Sec. III. Sec. IV investigates input-to-state stability of the proposed controller. Performance and evaluation of controller parameters is presented in Sec. V. A comparison with state-of-the-art controllers is summarized in Sec. VI. In Sec. VII, simulation and experimental results for a 3-DoF and a 7-DoF robotic arm are shown. Conclusions are drawn in Sec. VIII.

II. ADAPTIVE CONTROLLER

The dynamics of an n-link robot manipulator is expressed by the following Euler-Lagrange equations:

$$\boldsymbol{M}(\boldsymbol{q})\ddot{\boldsymbol{q}} + \boldsymbol{C}(\boldsymbol{q}, \dot{\boldsymbol{q}})\dot{\boldsymbol{q}} + \boldsymbol{G}(\boldsymbol{q}) + \boldsymbol{F}\dot{\boldsymbol{q}} = \boldsymbol{\tau}, \tag{1}$$

where $\boldsymbol{M}(\boldsymbol{q}) \in \mathbb{R}^{n\times n}$ is a symmetric positive definite inertia matrix, $\boldsymbol{C}(\boldsymbol{q}, \dot{\boldsymbol{q}}) \in \mathbb{R}^{n\times 1}$ is a matrix of centrifugal and Coriolis terms, $\boldsymbol{G} \in \mathbb{R}^{n\times 1}$ contains the gravitational terms acting

on the robot, $\boldsymbol{F} \in \mathbb{R}^{n\times n}$ is a diagonal matrix representing approximate values of viscous friction, $\boldsymbol{q} \in \mathbb{R}^{n\times 1}$ is a vector of joint angles and $\boldsymbol{\tau} \in \mathbb{R}^{n\times 1}$ is a vector of input torques applied at each joint. In the presence of external disturbances, $\boldsymbol{\tau} = \boldsymbol{\tau}_\mathrm{d} + \boldsymbol{\tau}_\mathrm{in}$, where $\boldsymbol{\tau}_\mathrm{d}$ is the disturbance term and $\boldsymbol{\tau}_\mathrm{in}$ is the input torque.

A. BACKGROUND

In an ideal scenario, where $\boldsymbol{\tau}_\mathrm{d} = \mathbf{0}$ and where the system dynamics are known, we can use feedback linearization, also called computed torque [8] for high-performance control. Let $\boldsymbol{N}(\boldsymbol{q}, \dot{\boldsymbol{q}}) = \boldsymbol{C}(\boldsymbol{q}, \dot{\boldsymbol{q}})\dot{\boldsymbol{q}} + \boldsymbol{G}(\boldsymbol{q})$ and

$$\boldsymbol{\tau} = \boldsymbol{M}\ddot{\boldsymbol{v}} + \boldsymbol{N}(\boldsymbol{q}, \dot{\boldsymbol{q}}) + \boldsymbol{F}\dot{\boldsymbol{q}}. \tag{2}$$

To achieve a desired transient and steady state response, let

$$\ddot{\boldsymbol{v}} = \ddot{\boldsymbol{q}}_\mathrm{d} - \boldsymbol{K}_\mathrm{d}\dot{\boldsymbol{e}} - \boldsymbol{K}_\mathrm{p}\boldsymbol{e}, \tag{3}$$

where $\boldsymbol{q}_\mathrm{d}$ is the reference trajectory, $\boldsymbol{e} = \boldsymbol{q} - \boldsymbol{q}_\mathrm{d}$, and $\boldsymbol{K}_\mathrm{d}$ and $\boldsymbol{K}_\mathrm{p} \in \mathbb{R}^{n\times n}$ are PD gains [7]. Substituting (2) and (3) into (1), we get the error dynamics

$$\ddot{\boldsymbol{e}} + \boldsymbol{K}_\mathrm{d}\dot{\boldsymbol{e}} + \boldsymbol{K}_\mathrm{p}\boldsymbol{e} = \mathbf{0}. \tag{4}$$

Simple pole-placement techniques can now attain the desired performance. Unfortunately, the system parameters often are not precisely known to achieve (4) and also external disturbances and un-modeled parameters are present in a real system.

B. ADAPTIVE COMPUTED-TORQUE CONTROLLER

The basic idea of the proposed controller is that the system dynamics can be represented by a vector $\boldsymbol{\phi}$. Theorem 1 is then used to find an estimate $\hat{\boldsymbol{\phi}}$ of $\boldsymbol{\phi}$, which is later used to calculate the input torque. The estimated system dynamics $\hat{\boldsymbol{\phi}}$ converges from zero to the real system dynamics, which is used for feedback linearization. Hence the controller can be seen as an adaptive computed-torque method. A thorough and complete proof of stability and robustness of the controller is given in Sec. III and IV. Here, we let $\boldsymbol{\phi}$ summarize the system dynamics:

$$\boldsymbol{\phi} = \boldsymbol{M}(\boldsymbol{q})\ddot{\boldsymbol{q}} + \boldsymbol{N}(\boldsymbol{q}, \dot{\boldsymbol{q}}) + \boldsymbol{F}\dot{\boldsymbol{q}} - \ddot{\boldsymbol{q}} - \boldsymbol{\tau}_\mathrm{d}, \tag{5}$$

where $\boldsymbol{\tau}_\mathrm{d}$ represents external disturbances and un-modeled dynamics [2], [15].

If the input torque is chosen as follows,

$$\boldsymbol{\tau}_\mathrm{in} = \hat{\boldsymbol{\phi}} + \ddot{\boldsymbol{q}}_\mathrm{d} - \boldsymbol{K}_\mathrm{d}\dot{\boldsymbol{e}} - \boldsymbol{K}_\mathrm{p}\boldsymbol{e} \tag{6}$$

with the assumption that the desired trajectory is twice differentiable, then by using (1), (5) and (6), we obtain the error dynamics

$$\ddot{\boldsymbol{e}} + \boldsymbol{K}_\mathrm{d}\dot{\boldsymbol{e}} + \boldsymbol{K}_\mathrm{p}\boldsymbol{e} = \hat{\boldsymbol{\phi}} - \boldsymbol{\phi}. \tag{7}$$

To find the input torque $\boldsymbol{\tau}_\mathrm{in}$, we need to evaluate $\hat{\boldsymbol{\phi}}$, which will be shown to be a function of only the state of the system (Sec. III). It is obvious here that if $\hat{\boldsymbol{\phi}} = \boldsymbol{\phi}$, we end up with (4), which is an ideal response. However, $\boldsymbol{\phi}$, which includes all the system dynamics along with disturbances in a single column (vector), is not known. The following Theorem provides the control law to obtain the estimate $\hat{\boldsymbol{\phi}}$.

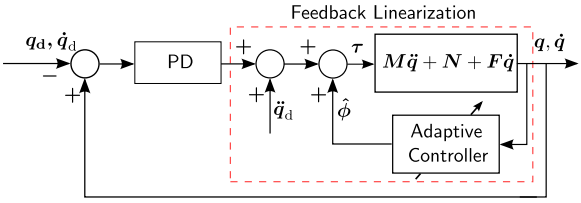

FIGURE 1. Adaptive Feedback linearization of robot manipulator.

Theorem 1 (Adaptation): Let $\tilde{\boldsymbol{\phi}} = \hat{\boldsymbol{\phi}} - \boldsymbol{\phi}$ and

$$\frac{\mathrm{d}^m\hat{\boldsymbol{\phi}}}{\mathrm{d}t^m} = -\sum_{i=0}^{m-1} a_i \frac{\mathrm{d}^i\tilde{\boldsymbol{\phi}}}{\mathrm{d}t^i}, \tag{8}$$

then the control law (6) leads to asymptotic stability of the joint error $\boldsymbol{e} = \mathbf{0}$ and estimation error $\tilde{\boldsymbol{\phi}} = \mathbf{0}$ for system (1).

Proof: The stability of the proposed adaptive law is proved in Sec. V. ■

The update law (8) does not require a regression matrix and can be implemented with low computational cost. The input torque $\boldsymbol{\tau}_\mathrm{in}$ is a function of only the state of the system (1), which is explained in Lemma 1 and also shown in (9) and (10). The constant coefficients a_i decide the rate of convergence of $\hat{\boldsymbol{\phi}}$ towards $\boldsymbol{\phi}$, explained in Sec. V-A.

Fig. 1 shows a block diagram representation of the proposed controller. The adaptive controller is applied in the inner loop and linearizes the overall feedback system. The reason for defining the controller as adaptive computed-torque is that, after $\hat{\boldsymbol{\phi}}$ converges to $\boldsymbol{\phi}$, the controller acts as a feedback linearization method.

Remark 1: For $m = 1$ and 2, the control laws are found by combining (7) and (8):

$$m = 1: \ \hat{\boldsymbol{\phi}} = -a_0\Big(\dot{\boldsymbol{e}} + \boldsymbol{K}_\mathrm{d}\boldsymbol{e} + \boldsymbol{K}_\mathrm{p}\int \boldsymbol{e}\,\mathrm{d}t\Big), \tag{9}$$

$$m = 2: \ \hat{\boldsymbol{\phi}} = -a_1(\dot{\boldsymbol{e}} + \boldsymbol{K}_\mathrm{d}\boldsymbol{e} + \boldsymbol{K}_\mathrm{p}\int \boldsymbol{e}\,\mathrm{d}t) - a_0(\boldsymbol{e} + \boldsymbol{K}_\mathrm{d}\int \boldsymbol{e}\,\mathrm{d}t + \boldsymbol{K}_\mathrm{p}\iint \boldsymbol{e}\,\mathrm{d}t^2). \tag{10}$$

Remark 2 (High-Frequency Problem): Adaptive controllers, in general, suffer from high-frequency noise during the transient-response. Fortunately, the motor drives and the power supplies act like low pass filters, and suppress the effect of noise.

Remark 3 (Noise): The only purpose of including $\ddot{\boldsymbol{q}}$ in (5) is to avoid the estimation of joint-acceleration when evaluating input torques.

Remark 4 (Approximation of $\boldsymbol{\phi}$): For a better estimation of $\boldsymbol{\phi}$, it is desired to select large m. However, the system will require large torques during the transient, which will be shown in the results section (VII). These high torques result in peaking which can affect the performance, see [38]. For that

reason, we have determined that $m = 2$ along with proper controller gains is sufficient to achieve desired performance.

Remark 5 (Tuning Parameters): The only tuning parameters are a_i, $\boldsymbol{K}_\mathrm{p}$ and $\boldsymbol{K}_\mathrm{d}$ and it will be shown in Sec. V how to select these controller parameters while satisfying a desired performance.

Remark 6: In our previous work [15], a term $\boldsymbol{f}(\boldsymbol{e}, \dot{\boldsymbol{e}})$ was included on the right-hand-side of (8) that was necessary for the stability proof. Fortunately, here a modified proof is presented that does not need this extra term.

III. ROBUSTNESS ANALYSIS

The proposed adaptive control method eventually constitutes an $\mathcal{H}_\infty$ robust-optimal controller. For a system to be robust, the $\mathcal{L}_2$-gain from disturbance to the performance index is less than or equal to some positive constant γ^2.

$$\frac{\int_\tau^\infty (\boldsymbol{x}^T \boldsymbol{Q}\boldsymbol{x} + \boldsymbol{u}^T \boldsymbol{R}\boldsymbol{u})\mathrm{d}t}{\int_\tau^\infty ||\boldsymbol{d}||^2 \mathrm{d}t} \leq \gamma^2, \tag{11}$$

where $\boldsymbol{Q}$ and $\boldsymbol{R}$ are positive definite matrices, $\boldsymbol{x}$ is a vector of states, $\boldsymbol{u}$ is the input and $\boldsymbol{d}$ is the disturbance. There also exists a smallest value $\gamma^* > 0$ such that (11) is satisfied for all $\gamma > \gamma^*$.

In this section, we will show that there exist matrices $\boldsymbol{Q}$ and $\boldsymbol{R}$ such that the system (1) along with the control law (8) satisfies the $\mathcal{L}_2$-gain condition (11). From the $\mathcal{H}_\infty$ perspective, the main idea is that we consider the system shown in Fig. 1 as a linear system with all the non-linearities, disturbances and unknown parameters as external disturbances as shown in Fig. 2. Thus, we can show robustness with respect to the unknown model. And finally, (8) results in a stable system as long as the system dynamics $\boldsymbol{\phi} \in \mathcal{L}_2[0, \infty)$. We start with a brief introduction of the $\mathcal{H}_\infty$ control method and the HJI equations.

A. $\mathcal{H}_\infty$ CONTROL

Solving the HJI equations for a non-linear system is a tedious task. Fortunately, if a robot manipulator is expressed in the following form:

$$\dot{\boldsymbol{x}} = \boldsymbol{A}\boldsymbol{x} \mathbin{\mathcal{C}} \boldsymbol{B}\boldsymbol{u} \mathbin{\mathcal{C}} \boldsymbol{D}\boldsymbol{d}, \tag{12}$$

then the HJI equation associated with the $\mathcal{L}_2$-gain (11) reduces to the game-algebraic Riccati equation [39]:

$$\boldsymbol{A}^T\boldsymbol{S} + \boldsymbol{S}\boldsymbol{A} - \boldsymbol{S}\boldsymbol{B}\boldsymbol{R}^{-1}\boldsymbol{B}^T\boldsymbol{S} + 1/\gamma^2 \boldsymbol{S}\boldsymbol{D}\boldsymbol{D}^T\boldsymbol{S} + \boldsymbol{Q} = \boldsymbol{0}. \tag{13}$$

Using $\boldsymbol{S}$ from (13), we obtain a static state feedback

$$\boldsymbol{u}^* = -\boldsymbol{R}^{-1}\boldsymbol{B}^T\boldsymbol{S}\boldsymbol{x} \triangleq -\boldsymbol{K}\boldsymbol{x}. \tag{14}$$

B. ROBUSTNESS PROOF

An inverse-optimal control method is used to prove the robustness of the proposed controller. Thus objective of this subsection is: *given the control law* (8)*, find the matrices* $\boldsymbol{S}$ *and* $\boldsymbol{Q}$ *such that the game-algebraic Riccati equation* (13) *is satisfied.*

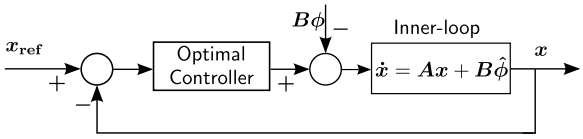

FIGURE 2. Adaptive controller from the perspective of $\mathcal{H}_\infty$ optimal controller.

The state-space form of the closed-loop equation for the Euler-Lagrange representation (7) can be written in the form of (12):

$$\dot{\boldsymbol{x}} = \boldsymbol{A}\boldsymbol{x} + \boldsymbol{B}\hat{\boldsymbol{\phi}} - \boldsymbol{B}\boldsymbol{\phi}, \tag{15}$$

Based on the value of m in (8), the matrices are

$$\begin{aligned}
\boldsymbol{A} &= \begin{bmatrix} \boldsymbol{0}_{(m+1)n\times n} & \boldsymbol{I}_{(m+1)n\times(m+1)n} \\ \boldsymbol{0}_{n\times n} & \boldsymbol{L}_{n\times(m+1)n} \end{bmatrix} \\
&\in \mathbb{R}^{(m+2)n\times(m+2)n}, \\
\boldsymbol{L} &= \begin{bmatrix} \boldsymbol{0}_{n\times(m-1)n} & -\boldsymbol{K}_\mathrm{p} - \boldsymbol{K}_\mathrm{d} \end{bmatrix} \in \mathbb{R}^{n\times(m+1)n}, \\
\boldsymbol{B} &= \begin{bmatrix} \boldsymbol{0}_{n\times(m+1)n} & \boldsymbol{I}_{n\times n} \end{bmatrix}^T \in \mathbb{R}^{(m+2)n\times 1}, \\
\boldsymbol{x} &= [\int_m \boldsymbol{e}^T \mathrm{d}t^m \quad \int_{m-1} \boldsymbol{e}^T \mathrm{d}t^{m-1} \quad \ldots \quad \boldsymbol{e}^T \quad \dot{\boldsymbol{e}}^T]^T,
\end{aligned}$$

where $\int_m$ represents the m^{th} integral with respect to time. Since $\hat{\boldsymbol{\phi}}$ determines the input torque according to (6), we can consider $-\boldsymbol{\phi}$ as disturbance '$\boldsymbol{d}$'. In the remainder of this paper, we will use the conventional input symbol '$\boldsymbol{u}$' and disturbance '$\boldsymbol{d}$' variables interchangeably for '$\hat{\boldsymbol{\phi}}$' and '$-\boldsymbol{\phi}$' respectively. The following lemma describes a different representation of (8) that will make it possible to apply the HJI equation on our system.

Lemma 1 (Alternative Form for (8)*):* Let

$$\hat{\boldsymbol{\phi}} = -\sum_{i=1}^{m+2} \Big(a_{i-1}\boldsymbol{K}_\mathrm{p} + a_{i-2}\boldsymbol{K}_\mathrm{d} + a_{i-3}\Big)\boldsymbol{x}[i] \triangleq -\boldsymbol{K}\boldsymbol{x}, \tag{16}$$

where $\boldsymbol{x}[i]$ is the i^{th} element of the state vector, with the condition

$$\mathrm{E1}: a_i = 0 \quad \forall\, i < 0,\ i > m-1.$$

Then (16) is equivalent to (8).

Proof: Equation (16) can be rearranged by taking advantage of condition E1 to get the following form:

$$\hat{\boldsymbol{\phi}} = -\sum_{i=1}^{m+2} \Big(a_{i-1}\boldsymbol{K}_\mathrm{p}\boldsymbol{x}[i] + a_{i-1}\boldsymbol{K}_\mathrm{d}\boldsymbol{x}[i+1] + a_{i-1}\boldsymbol{x}[i+2]\Big),$$

$$\hat{\boldsymbol{\phi}} = -\sum_{i=1}^{m} a_{i-1}\Big(\boldsymbol{K}_\mathrm{p}\boldsymbol{x}[i] + \boldsymbol{K}_\mathrm{d}\boldsymbol{x}[i+1] + \boldsymbol{x}[i+2]\Big),$$

Integrating (7), we get

$$\int_{m-i+1} \tilde{\boldsymbol{\phi}} = \boldsymbol{K}_\mathrm{p}\boldsymbol{x}[i] + \boldsymbol{K}_\mathrm{d}\boldsymbol{x}[i+1] + \boldsymbol{x}[i+2]. \tag{17}$$

Taking the m^{th} derivative, we get the control law (8). ■

$$\boldsymbol{Q} = \begin{bmatrix} \tilde{\boldsymbol{K}} b_0^2 \boldsymbol{K}_\mathrm{p}^2 & \boldsymbol{0} & \boldsymbol{0} & \boldsymbol{0} \\ \boldsymbol{0} & \tilde{\boldsymbol{K}} b_0^2 (\boldsymbol{K}_\mathrm{d}^2 - 2\boldsymbol{K}_\mathrm{p}) + \boldsymbol{K}_\mathrm{p}^2 (\tilde{\boldsymbol{K}} - 2b_0 \boldsymbol{I}) & \boldsymbol{0} & \boldsymbol{0} \\ \boldsymbol{0} & \boldsymbol{0} & \tilde{\boldsymbol{K}} b_0^2 + (\tilde{\boldsymbol{K}} - 2b_0 \boldsymbol{I})(\boldsymbol{K}_\mathrm{d}^2 - 2\boldsymbol{K}_\mathrm{p}) & \boldsymbol{0} \\ \boldsymbol{0} & \boldsymbol{0} & \boldsymbol{0} & \tilde{\boldsymbol{K}} - 2b_0 \boldsymbol{I} \end{bmatrix}, \quad b_0 = \frac{a_0}{a_1}$$

$$\boldsymbol{S} = \begin{bmatrix} b_0 \tilde{\boldsymbol{K}} \boldsymbol{K}_\mathrm{p}^2 + b_0^2 \tilde{\boldsymbol{K}} \boldsymbol{K}_\mathrm{p} \boldsymbol{K}_\mathrm{d} & b_0 \boldsymbol{K}_\mathrm{p}^2 + b_0^2 \tilde{\boldsymbol{K}} \boldsymbol{K}_\mathrm{p} + b_0 \tilde{\boldsymbol{K}} \boldsymbol{K}_\mathrm{p} \boldsymbol{K}_\mathrm{d} & b_0 \tilde{\boldsymbol{K}} \boldsymbol{K}_\mathrm{p} + b_0 \boldsymbol{K}_\mathrm{p} \boldsymbol{K}_\mathrm{d} & b_0 \boldsymbol{K}_\mathrm{p} \\ b_0 \boldsymbol{K}_\mathrm{p}^2 + b_0^2 \tilde{\boldsymbol{K}} \boldsymbol{K}_\mathrm{p} + b_0 \tilde{\boldsymbol{K}} \boldsymbol{K}_\mathrm{p} \boldsymbol{K}_\mathrm{d} & b_0^2 \tilde{\boldsymbol{K}} \boldsymbol{K}_\mathrm{d} + b_0 \tilde{\boldsymbol{K}} \boldsymbol{K}_\mathrm{d}^2 + \tilde{\boldsymbol{K}} \boldsymbol{K}_\mathrm{p} \boldsymbol{K}_\mathrm{d} + \boldsymbol{K}_\mathrm{p}^2 & b_0 \boldsymbol{K}_\mathrm{d}^2 + \tilde{\boldsymbol{K}} \boldsymbol{K}_\mathrm{p} + b_0 \tilde{\boldsymbol{K}} \boldsymbol{K}_\mathrm{d} + \boldsymbol{K}_\mathrm{p} \boldsymbol{K}_\mathrm{d} - b_0 \boldsymbol{K}_\mathrm{p} & \boldsymbol{K}_\mathrm{p} + b_0 \boldsymbol{K}_\mathrm{d} \\ b_0 \tilde{\boldsymbol{K}} \boldsymbol{K}_\mathrm{p} + b_0 \boldsymbol{K}_\mathrm{p} \boldsymbol{K}_\mathrm{d} & b_0 \boldsymbol{K}_\mathrm{d}^2 + \tilde{\boldsymbol{K}} \boldsymbol{K}_\mathrm{p} + b_0 \tilde{\boldsymbol{K}} \boldsymbol{K}_\mathrm{d} + \boldsymbol{K}_\mathrm{p} \boldsymbol{K}_\mathrm{d} - b_0 \boldsymbol{K}_\mathrm{p} & \boldsymbol{K}_\mathrm{d}^2 + b_0 \tilde{\boldsymbol{K}} + \tilde{\boldsymbol{K}} \boldsymbol{K}_\mathrm{d} & \boldsymbol{K}_\mathrm{d} + b_0 \boldsymbol{I} \\ b_0 \boldsymbol{K}_\mathrm{p} & \boldsymbol{K}_\mathrm{p} + b_0 \boldsymbol{K}_\mathrm{d} & \boldsymbol{K}_\mathrm{d} + b_0 \boldsymbol{I} & \boldsymbol{I} \end{bmatrix} \tag{18}$$

Remark 7: For second-order ($m = 2$), the controller (16) can be written as

$$\frac{\mathrm{d}^2 \hat{\boldsymbol{\phi}}}{\mathrm{d}t^2} = -a_1 \frac{\mathrm{d}}{\mathrm{d}t} (\ddot{\boldsymbol{e}} + \boldsymbol{K}_\mathrm{d} \dot{\boldsymbol{e}} + \boldsymbol{K}_\mathrm{p} \boldsymbol{e}) - a_0 (\ddot{\boldsymbol{e}} + \boldsymbol{K}_\mathrm{d} \dot{\boldsymbol{e}} + \boldsymbol{K}_\mathrm{p} \boldsymbol{e}). \tag{19}$$

It is obvious from the example $m = 1$ in (9) and $m = 2$ in (10) that $\hat{\boldsymbol{\phi}}$ can be written as a state feedback $\hat{\boldsymbol{\phi}} = -\boldsymbol{K}\boldsymbol{x}$ with appropriate choice of $\boldsymbol{K}$. The general case is treated in lemma 1. This will allow us a comparison of (14) and (16). The next Theorem gives the optimality of the proposed adaptive control method for the appropriate choice of $\boldsymbol{R}$ and $\boldsymbol{Q}$. Here, only the matrices $\boldsymbol{S}$ and $\boldsymbol{Q}$ are evaluated using inverse-optimal control.

Remark 8: The matrix $\boldsymbol{R}$ is chosen as

$$\boldsymbol{R}^{-1} = \alpha \tilde{\boldsymbol{K}} + \boldsymbol{I}/\gamma^2 \triangleq a_{m-1} \boldsymbol{I}, \quad \alpha > \boldsymbol{0},\ \tilde{\boldsymbol{K}} > \boldsymbol{0}, \tag{20}$$

which is proved by ISS (Sec. V).

For proving the optimal robustness, $m = 2$ is assumed. The reason is that there is no generalized procedure to proof the robustness for all m. But fortunately, the proof can be extended for any value of m. Another intuition for $m = 2$ is explained in Sec. VII-C.

Theorem 2 (Robust-Optimal Controller $m = 2$): For a system (15), the proposed adaptive controller (10) or (19) gives an optimal solution that satisfies the game-algebraic Riccati equation (13) under the following conditions:

- A1: a_0, a_1, $\boldsymbol{K}_\mathrm{p}$ and $\boldsymbol{K}_\mathrm{d} > \boldsymbol{0}$
- A2: $\boldsymbol{K}_\mathrm{d}^2 > 2\boldsymbol{K}_\mathrm{p}$
- A3: $a_1 \tilde{\boldsymbol{K}} > 2a_0 \boldsymbol{I}$

Proof: If the above controller (19) is optimal, that means it satisfies the $\mathcal{L}_2$-gain condition of (11), there exist $\boldsymbol{Q}$, $\boldsymbol{R}$ and $\boldsymbol{S}$ symmetric, positive definite satisfying (13).

To find the values of $\boldsymbol{Q}$ and $\boldsymbol{S}$, we follow the steps below:

- assume $\boldsymbol{Q}$ to be a diagonal matrix
- find the last column/row of matrix $\boldsymbol{S}$ using $-\boldsymbol{K}\boldsymbol{x} = -\boldsymbol{R}^{-1}\boldsymbol{B}^T\boldsymbol{S}\boldsymbol{x}$
- find the remaining entries of $\boldsymbol{S}$ and diagonal elements of $\boldsymbol{Q}$ using (13), see (18), as shown at the top of this page.

From the $\boldsymbol{Q}$ matrix (18), required to be positive definite, we can deduce conditions A1-A3. ■

There exists more than one solution for $\boldsymbol{Q}$ and $\boldsymbol{S}$ that fulfills the positive definiteness criterion, but using the form (16) and (20), after some mathematical manipulation, we can evaluate the matrices (18). To facilitate the analysis, we assume $\alpha = 1$ as explained in Sec. IV-B.

Since the control law satisfies the Hamilton-Jacobi-Bellman equation, we can conclude that the $\mathcal{L}_2$-gain is always less than γ. From the definition of the $\mathcal{L}_2$-gain problem, it is also clear that the system remains stable for $\boldsymbol{\phi} \in \mathcal{L}_2[0, \infty)$ [39]. In the results section, it will be shown that A2 is a sufficient condition but not necessary for stability. For $m = 2$, $\boldsymbol{K}$ can be written as

$$\boldsymbol{K} = a_1 [b_0 \boldsymbol{K}_\mathrm{p} \quad \boldsymbol{K}_\mathrm{p} + b_0 \boldsymbol{K}_\mathrm{d} \quad \boldsymbol{K}_\mathrm{d} + b_0 \boldsymbol{I} \quad \boldsymbol{I}], \tag{21}$$

where $b_0 = a_0/a_1$. The reason for writing the a_1 out of $\boldsymbol{B}^T\boldsymbol{S}\boldsymbol{x}$ is that $\boldsymbol{R}^{-1} = a_1\boldsymbol{I}$, see Sec. IV. Disturbance attenuation depends on the value of γ that is included in the $\boldsymbol{R}^{-1}$ matrix.

Remark 9 (Special Case): For a first order approximation, that is $m = 1$, the robust-adaptive controller proposed in this paper is similar to the $\mathcal{H}_\infty$ inverse-optimal Controller [5], [12]. The $\boldsymbol{Q}$ matrix in this case is

$$\boldsymbol{Q} = \begin{bmatrix} \tilde{\boldsymbol{K}} \boldsymbol{K}_\mathrm{p}^2 & \boldsymbol{0} & \boldsymbol{0} \\ \boldsymbol{0} & \tilde{\boldsymbol{K}} (\boldsymbol{K}_\mathrm{d}^2 - 2\boldsymbol{K}_\mathrm{p}) & \boldsymbol{0} \\ \boldsymbol{0} & \boldsymbol{0} & \tilde{\boldsymbol{K}} \end{bmatrix}. \tag{22}$$

The conditions for this $\boldsymbol{Q}$ matrix are

- B1: a_0, $\boldsymbol{K}_\mathrm{p}$ and $\boldsymbol{K}_\mathrm{d} > 0$
- B2: $\boldsymbol{K}_\mathrm{d}^2 > 2\boldsymbol{K}_\mathrm{p}$

If we let $a_0\boldsymbol{I} = \boldsymbol{R}^{-1}$ where $\boldsymbol{R}^{-1}$ is given by equation (20), then the control law is represented as (9), which is equivalent to the controller proposed by Choi *et al.* [12]. Of course $\hat{\boldsymbol{\phi}} \neq \boldsymbol{\tau}_\mathrm{in}$, so the controllers are not exactly equal. Because of that, the performance analysis is different, and we can show that the mismatch approaches zero. Similar to that $\mathcal{H}_\infty$ controller, the proposed adaptive control method can be applied on a robot manipulator without any knowledge about the system dynamics.

IV. INPUT-TO-STATE-STABILITY

So far, we have discussed the robustness using the $\mathcal{H}_\infty$ approach. In this section, we use ISS to derive the proposed controller (8) along with stability and the matrix $\boldsymbol{R}$ (20), which we have used in Theorem 2. We start with a brief introduction to ISS.

A. BACKGROUND

For a linear system, the bounded-input-bounded-output stability is not affected by inputs or disturbances provided that they are bounded. However, for non-linear systems, an internally stable system can become unstable if certain inputs are applied. Because of that, Sontag proposed a definition called input-to-state-stability that also considers inputs to find the stability of a non-linear system [40]–[42]. Because disturbances and model uncertainties can be considered as part of input disturbance, ISS can also be used to find the stability and robustness of a system.

For a general non-linear control system

$$\dot{\boldsymbol{x}} = \boldsymbol{f}(\boldsymbol{x}, \boldsymbol{d}), \tag{23}$$

where $\boldsymbol{x}$ and $\boldsymbol{d}$ are the state and disturbance vectors, respectively: the ISS stability is defined as

$$|\boldsymbol{x}(t)| \leq \beta(|\boldsymbol{x}(0)|, t) + \gamma(||\boldsymbol{d}||_\infty), \quad \forall t \geq 0, \tag{24}$$

where $\beta \in \mathcal{KL}$, $\gamma \in \mathcal{K}_\infty$ [42] and $\boldsymbol{x}(0)$ is the initial state. A class $\mathcal{K}_\infty$ is a function $\alpha : \mathbb{R}_{\geq 0} \to \mathbb{R}_{\geq 0}$, which is continuous, unbounded, increasing and satisfies $\alpha(0) = 0$. A class $\mathcal{KL}$ is a function $\beta : \mathbb{R}_{\geq 0} \times \mathbb{R}_{\geq 0} \to \mathbb{R}_{\geq 0}$, such that $\beta(., t) \in \mathcal{K}_\infty$ for all t and $\beta(r, t) \searrow 0$ as $t \to \infty$, where r is a constant.

In case of a linear system, we get

$$\beta(t) = |\boldsymbol{x}(0)|\, ||e^{\boldsymbol{A}t}||, \quad \gamma = ||\boldsymbol{B}|| \int_0^\infty ||e^{\boldsymbol{A}t}|| \mathrm{d}\tau. \tag{25}$$

A result that will later be used to find the control law is given in [42]: "*A system is ISS if and only if it admits a smooth ISS-Lyapunov function*". That means that there exists a positive definite function $V(\boldsymbol{x}) \in \mathbb{R}$ and $\alpha_1, \alpha_2 \in \mathcal{K}_\infty$ such that

$$\alpha_1(|\boldsymbol{x}|) \leq V(\boldsymbol{x}) \leq \alpha_2(|\boldsymbol{x}|). \tag{26}$$

ISS stability of (23) can then be concluded from

$$\dot{V}(\boldsymbol{x}) \leq -\gamma_1(|\boldsymbol{x}|) + \gamma_2(|\boldsymbol{d}|), \quad \forall\, \boldsymbol{x}, \boldsymbol{d}, \tag{27}$$

where $\gamma_{(.)} \in \mathcal{K}_\infty$. Further, let there exist $V(\boldsymbol{x})$ such that the following condition is satisfied for all $\boldsymbol{x}$ and $\boldsymbol{u}$ [36]:

$$|\boldsymbol{x}| \geq \rho(|\boldsymbol{d}|) \Rightarrow \dot{V}(\boldsymbol{x}) \leq -\gamma_3(|\boldsymbol{x}|), \tag{28}$$

where γ_3 and $\rho \in \mathcal{K}_\infty$. In this case, not only is the system ISS but also asymptotically stable.

B. DERIVATION OF PROPOSED CONTROLLER

To obtain the control law, the basic idea here is to consider $\boldsymbol{u} = \hat{\boldsymbol{\phi}}$ and use equation (28) as explained in the next Theorem.

Theorem 3 (Derivation): For the control law

$$\hat{\boldsymbol{\phi}} = -\Big(\alpha\tilde{\boldsymbol{K}} + \frac{\rho^{-1}(|\boldsymbol{x}|)}{|\boldsymbol{x}_\triangle|}\Big)\boldsymbol{x}_\triangle, \quad \tilde{\boldsymbol{K}} > \boldsymbol{0}, \tag{29}$$

the system (15) is ISS, where $\rho \in \mathcal{K}_\infty$, $\alpha > 1/2$ and $\boldsymbol{x}_\triangle$ is

$$b_0\boldsymbol{K}_\mathrm{p}\boldsymbol{x}[1] + (b_0\boldsymbol{K}_\mathrm{d} + \boldsymbol{K}_\mathrm{p})\boldsymbol{x}[2] + (b_0\boldsymbol{I} + \boldsymbol{K}_\mathrm{d})\boldsymbol{x}[3] + \boldsymbol{x}[4],$$

which is equal to $\boldsymbol{B}^T\boldsymbol{S}\boldsymbol{x}$. Also there exists an ISS-Lyapunov function

$$V(\boldsymbol{x}) = \frac{1}{2}\boldsymbol{x}^T\boldsymbol{S}\boldsymbol{x} \tag{30}$$

with $\boldsymbol{S}$ from (18) and if conditions A1-A3 are satisfied.

Proof: For the stability of (15), the derivative of the Lyapunov function has to satisfy the following condition:

$$\dot{V}(\boldsymbol{x}) = \nabla V\boldsymbol{A}\boldsymbol{x} + \nabla V\boldsymbol{B}\hat{\boldsymbol{\phi}} - \nabla V\boldsymbol{B}\boldsymbol{\phi} \leq 0. \tag{31}$$

$\nabla V\boldsymbol{A}\boldsymbol{x}$ from (31) can be rewritten as

$$\begin{aligned}\nabla V\boldsymbol{A}\boldsymbol{x} &= \frac{1}{2}\boldsymbol{x}^T(\boldsymbol{A}^T\boldsymbol{S} + \boldsymbol{S}\boldsymbol{A})\boldsymbol{x}, \\ &= \frac{1}{2}\Big[\tilde{\boldsymbol{K}}\boldsymbol{x}_\triangle^T\boldsymbol{x}_\triangle - \boldsymbol{x}^T[4](\tilde{\boldsymbol{K}} - 2b_0\boldsymbol{I})\boldsymbol{x}[4] \\ &\quad - \boldsymbol{x}^T[2]\Big(\tilde{\boldsymbol{K}}b_0^2(\boldsymbol{K}_\mathrm{d}^2 - 2\boldsymbol{K}_\mathrm{p}) + \boldsymbol{K}_\mathrm{p}^2(\tilde{\boldsymbol{K}} - 2b_0\boldsymbol{I})\Big)\boldsymbol{x}[2] \\ &\quad - \boldsymbol{x}^T[3]\Big((\tilde{\boldsymbol{K}} - 2b_0\boldsymbol{I})(\boldsymbol{K}_\mathrm{d}^2 - 2\boldsymbol{K}_\mathrm{p}) + \tilde{\boldsymbol{K}}b_0^2\Big)\boldsymbol{x}[3]\Big].\end{aligned} \tag{32}$$

and

$$\nabla V_x\boldsymbol{B} = \boldsymbol{x}^T\boldsymbol{S}\boldsymbol{B} \triangleq \boldsymbol{x}_\triangle^T, \tag{33}$$

$\dot{V} < 0$ is thus satisfied if

$$\begin{aligned}&\frac{1}{2}\tilde{\boldsymbol{K}}\boldsymbol{x}_\triangle^T\boldsymbol{x}_\triangle + \boldsymbol{x}_\triangle\hat{\boldsymbol{\phi}} - \boldsymbol{x}_\triangle\boldsymbol{\phi} \\ &\quad \leq \frac{1}{2}\Big[\boldsymbol{x}^T[2]\Big(\tilde{\boldsymbol{K}}b_0^2(\boldsymbol{K}_\mathrm{d}^2 - 2\boldsymbol{K}_\mathrm{p}) + \boldsymbol{K}_\mathrm{p}^2(\tilde{\boldsymbol{K}} - 2b_0\boldsymbol{I})\Big)\boldsymbol{x}[2] \\ &\qquad + \boldsymbol{x}^T[3]\Big((\tilde{\boldsymbol{K}} - 2b_0\boldsymbol{I})(\boldsymbol{K}_\mathrm{d}^2 - 2\boldsymbol{K}_\mathrm{p}) + \tilde{\boldsymbol{K}}b_0^2\Big)\boldsymbol{x}[3] \\ &\qquad + \boldsymbol{x}^T[4](\tilde{\boldsymbol{K}} - 2b_0\boldsymbol{I})\boldsymbol{x}[4]\Big].\end{aligned} \tag{34}$$

From the above equation, if conditions A1-A3 from Theorem 2 are satisfied, then the right-hand side of (34) is positive. To prove that the Lyapunov function (31) is an ISS-Lyapunov function, the left-hand side of (34) must be at least negative semi-definite. Taking advantage of (28), we get:

$$\frac{\tilde{\boldsymbol{K}}}{2}\boldsymbol{x}_\triangle^T\boldsymbol{x}_\triangle + \boldsymbol{x}_\triangle\hat{\boldsymbol{\phi}} - \boldsymbol{x}_\triangle\boldsymbol{\phi} \leq \frac{\tilde{\boldsymbol{K}}}{2}\boldsymbol{x}_\triangle^T\boldsymbol{x}_\triangle + \boldsymbol{x}_\triangle\hat{\boldsymbol{\phi}} + |\boldsymbol{x}_\triangle|\rho^{-1}(|\boldsymbol{x}|). \tag{35}$$

To make sure that the above equation is negative definite or semi-definite, $\hat{\boldsymbol{\phi}}$ is chosen as

$$\hat{\boldsymbol{\phi}} = -\Big(\alpha\tilde{\boldsymbol{K}} + \frac{\rho^{-1}(|\boldsymbol{x}|)}{|\boldsymbol{x}_\triangle|}\boldsymbol{I}\Big)\boldsymbol{x}_\triangle. \tag{36}$$

■

Remark 10 (Special Case [12]): For $m = 1$, we get a similar solution as suggested by Choi *et al.* [12].

C. EVALUATION OF THE MATRIX R

It is now obvious, how $\boldsymbol{R}$ has to be chosen. Comparing (14) and (29), we get

$$\boldsymbol{R}^{-1} = (\alpha\tilde{\boldsymbol{K}} + \frac{\rho^{-1}(|\boldsymbol{x}|)}{|\boldsymbol{x}_\triangle|}\boldsymbol{I}). \tag{37}$$

To show the $\mathcal{H}_\infty$ optimality for the proposed controller, we choose the following performance index [39]:

$$J = \int_0^t \boldsymbol{x}^T \boldsymbol{Q}\boldsymbol{x} + \boldsymbol{u}^T \boldsymbol{R}\boldsymbol{u} - \gamma^2 \boldsymbol{d}^T \boldsymbol{d}\, \mathrm{d}\tau \tag{38}$$

To proof the optimality of the robust-adaptive controller, we use inverse-optimal control as explained in [36]. For $m = 1$, the inverse-optimality is also proved in [5] and [12]. The above performance equation as explained in Sec. III-A requires the HJI (13) equation to be solved.

Theorem 4 (Optimality [12]): For a control law (36), applied to a robot manipulator (1), we get an optimal solution if the following condition is satisfied

$$\frac{\rho^{-1}(|\boldsymbol{x}|)}{|\boldsymbol{x}_\triangle|} = \frac{1}{\gamma^2},$$

where without loss of generality $\alpha = 1$ is considered for simplicity.

Proof: It is already proved under conditions A1-A3 that matrix $\boldsymbol{Q}$ (18) is positive definite. Condition 2 is evident because we select $\boldsymbol{R}^{-1}$ such that $1/\gamma^2$ cancels out the disturbance term. The HJI equations can be used in the performance equation (38) as:

$$\begin{aligned}
J(\boldsymbol{x}) &= -\lim_{t\to\infty} \int_0^t \boldsymbol{x}^T(\boldsymbol{A}^T\boldsymbol{S} + \boldsymbol{S}\boldsymbol{A} - \boldsymbol{S}\boldsymbol{B}\tilde{\boldsymbol{K}}\boldsymbol{B}^T\boldsymbol{S})\boldsymbol{x}\, \mathrm{d}\tau \\
&\quad + \int_0^t \boldsymbol{u}^T\boldsymbol{R}\boldsymbol{u} - \gamma^2\boldsymbol{d}^T\boldsymbol{d}\, \mathrm{d}\tau, \\
&= -\int_0^\infty \boldsymbol{x}^T(\boldsymbol{A}^T\boldsymbol{S} + \boldsymbol{S}\boldsymbol{A})\boldsymbol{x} + 2\boldsymbol{x}^T\boldsymbol{S}\boldsymbol{B}\boldsymbol{u}\, \mathrm{d}\tau \\
&\quad + \int_0^\infty \boldsymbol{u}^T\boldsymbol{R}\boldsymbol{u} + 2\boldsymbol{x}^T\boldsymbol{S}\boldsymbol{B}\boldsymbol{u}\; \mathcal{C}\; \boldsymbol{x}^T\boldsymbol{S}\boldsymbol{B}\tilde{\boldsymbol{K}}\boldsymbol{B}^T\boldsymbol{S}\boldsymbol{x}\, \mathrm{d}\tau \\
&\quad + \int_0^\infty -\gamma^2\boldsymbol{d}^T\boldsymbol{d} + 2\boldsymbol{x}^T\boldsymbol{S}\boldsymbol{B}\boldsymbol{d} - 2\boldsymbol{x}^T\boldsymbol{S}\boldsymbol{B}\boldsymbol{d}\, \mathrm{d}\tau \\
&= -\int_0^\infty 2V_{\boldsymbol{x}}\boldsymbol{A}\boldsymbol{x} + 2V_{\boldsymbol{x}}\boldsymbol{B}\boldsymbol{u} + 2V_{\boldsymbol{x}}\boldsymbol{B}\boldsymbol{d}\, \mathrm{d}\tau \\
&\quad + \int_0^\infty (\boldsymbol{u} + \boldsymbol{R}^{-1}\boldsymbol{B}^T\boldsymbol{S}\boldsymbol{x})^T\boldsymbol{R}(\boldsymbol{u} + \boldsymbol{R}^{-1}\boldsymbol{B}^T\boldsymbol{S}\boldsymbol{x})\, \mathrm{d}\tau \\
&\quad - \gamma^2\int_0^\infty (\boldsymbol{d} - \frac{1}{\gamma^2}\boldsymbol{B}^T\boldsymbol{S}\boldsymbol{x})^T(\boldsymbol{d} - \frac{1}{\gamma^2}\boldsymbol{B}^T\boldsymbol{S}\boldsymbol{x})\, \mathrm{d}\tau, \\
&\quad - \int_0^\infty (\frac{\rho^{-1}(|\boldsymbol{x}|)}{|\boldsymbol{x}_\triangle|} - \frac{1}{\gamma^2})\boldsymbol{x}^T\boldsymbol{S}\boldsymbol{B}\boldsymbol{B}^T\boldsymbol{S}\boldsymbol{x}\, \mathrm{d}\tau, \\
&= -2V(\boldsymbol{x}(0)) + \\
&\quad - \int_0^\infty (\boldsymbol{u} + \boldsymbol{R}^{-1}\boldsymbol{B}^T\boldsymbol{S}\boldsymbol{x})^T\boldsymbol{R}(\boldsymbol{u} + \boldsymbol{R}^{-1}\boldsymbol{B}^T\boldsymbol{S}\boldsymbol{x})\, \mathrm{d}\tau \\
&\quad - \gamma^2\int_0^\infty (\boldsymbol{d} - \frac{1}{\gamma^2}\boldsymbol{B}^T\boldsymbol{S}\boldsymbol{x})^T(\boldsymbol{d} - \frac{1}{\gamma^2}\boldsymbol{B}^T\boldsymbol{S}\boldsymbol{x})\, \mathrm{d}\tau, \\
&\quad - \int_0^\infty (\frac{\rho^{-1}(|\boldsymbol{x}|)}{|\boldsymbol{x}_\triangle|} - \frac{1}{\gamma^2})|\boldsymbol{x}_\triangle|^2\, \mathrm{d}\tau.
\end{aligned}$$

In the last step, we assume that the final state fulfills $V(\boldsymbol{x}(\infty)) = 0$. Considering $\boldsymbol{u}$ to be equal to (14), we get the optimal solution with respect to the performance index mentioned above. Note that

$$\boldsymbol{d} = \frac{1}{\gamma^2}\boldsymbol{B}^T\boldsymbol{S}\boldsymbol{x}$$

is the worst case disturbance as explained in [39]. To achieve the minimum cost function, the following should be satisfied:

$$\frac{\rho^{-1}(|\boldsymbol{x}|)}{|\boldsymbol{x}_\triangle|} = \frac{1}{\gamma^2}.$$

Hence it is proved that

$$\boldsymbol{R}^{-1} = \tilde{\boldsymbol{K}} + \frac{\rho^{-1}(|\boldsymbol{x}|)}{|\boldsymbol{x}_\triangle|}\boldsymbol{I} = \tilde{\boldsymbol{K}} + \frac{\boldsymbol{I}}{\gamma^2}$$

gives the optimal solution. By considering $\boldsymbol{R}^{-1} = a_{m-1}\boldsymbol{I}$, we get to the proposed controller from Theorem 1. ■

V. PERFORMANCE ANALYSIS AND STABILITY

In this section, the primary focus is to discuss and quantify the performance of the controller. Then based on a performance criterion, the parameters of the proposed controller are evaluated. The performance criterion in this paper is an upper bound on the absolute values of the joint errors at steady state. This approach is explained in the next Theorem.

Theorem 5 (Performance): For the control law

$$\hat{\boldsymbol{\phi}} = \Big(\tilde{\boldsymbol{K}} + \frac{\boldsymbol{I}}{\gamma^2}\Big)\boldsymbol{x}_\triangle, \quad \boldsymbol{x}_\triangle = \boldsymbol{B}^T\boldsymbol{S}\boldsymbol{x} \tag{39}$$

with the conditions given in Theorem 2, the performance limitation is given as:

$$|\boldsymbol{x}|_{\mathrm{P,L}} \leq \frac{2\boldsymbol{S}\boldsymbol{B}}{\lambda_{\min}}|\boldsymbol{\phi}_{\max}|, \tag{40}$$

where

$$\lambda_{min} = \lambda_{min}\Big(\boldsymbol{Q} + (2a_{m-1} - \tilde{\boldsymbol{K}})\boldsymbol{S}\boldsymbol{B}\boldsymbol{B}^T\boldsymbol{S}\Big),$$

and $|\boldsymbol{x}|_{\mathrm{P,L}}$ is the maximum allowed error in steady state.

Proof: The derivative of the Lyapunov function (30) is given as

$$\dot{V} = \frac{1}{2}\boldsymbol{x}^T(\boldsymbol{A}^T\boldsymbol{S} + \boldsymbol{S}\boldsymbol{A})\boldsymbol{x} + \boldsymbol{x}^T\boldsymbol{S}\boldsymbol{B}\tilde{\boldsymbol{\phi}}. \tag{41}$$

The above equation can also be written as

$$\begin{aligned}
\dot{V} &= \frac{1}{2}\boldsymbol{x}^T(\boldsymbol{A}^T\boldsymbol{S} + \boldsymbol{S}\boldsymbol{A} - \boldsymbol{S}\boldsymbol{B}\tilde{\boldsymbol{K}}\boldsymbol{B}\boldsymbol{S})\boldsymbol{x} \\
&\quad + \frac{1}{2}\boldsymbol{x}^T\boldsymbol{S}\boldsymbol{B}\tilde{\boldsymbol{K}}\boldsymbol{B}^T\boldsymbol{S}\boldsymbol{x} + \boldsymbol{x}^T\boldsymbol{S}\boldsymbol{B}\tilde{\boldsymbol{\phi}},
\end{aligned}$$

Applying (39), we get

$$\tilde{\boldsymbol{\phi}} = -\boldsymbol{R}^{-1}\boldsymbol{B}^T\boldsymbol{S}\boldsymbol{x} - \int_m \frac{\mathrm{d}^m\boldsymbol{\phi}}{\mathrm{d}t}.$$

For the sake of simplicity, let $\tilde{K}$ be a scalar quantity. The derivative of the Lyapunov function is

$$\dot{V} = -\frac{1}{2}\boldsymbol{x}^T(\boldsymbol{Q} + (2a_{m-1} - \tilde{K})\boldsymbol{S}\boldsymbol{B}\boldsymbol{B}^T\boldsymbol{S})\boldsymbol{x} - \boldsymbol{x}^T\boldsymbol{S}\boldsymbol{B}\int_m \frac{\mathrm{d}^m\boldsymbol{\phi}}{\mathrm{d}t}, \tag{42}$$

where $a_{m-1}\boldsymbol{I} = \boldsymbol{R}^{-1}$. To find the performance limitation of the controller in terms of errors, (42) can be written as

$$\dot{V} \leq -\frac{1}{2}\lambda_{min}\boldsymbol{x}^T\boldsymbol{x} - \boldsymbol{x}^T\boldsymbol{S}\boldsymbol{B}\boldsymbol{\phi}. \tag{43}$$

According to that, $\dot{V} < 0$ is possible if and only if

$$|\boldsymbol{x}| \leq \frac{2\boldsymbol{SB}}{\lambda_{min}}|\boldsymbol{\phi}_{\max}|.$$

This also proofs Theorem 1. ∎

Remark 11: The disturbance term $\boldsymbol{\phi}$ is a function of $\boldsymbol{q}, \dot{\boldsymbol{q}}$ and $\ddot{\boldsymbol{q}}$. It is relatively easy to find the estimate of the maximum value of $|\boldsymbol{\phi}|$, so to ensure that the joint errors never exceed a predefined value. For that reason, the above equation must be satisfied. From equation (43), it can also be concluded that the proposed control method is indeed ISS.

A. EVALUATION OF CONTROLLER PARAMETERS

After discussing the performance limitation, the next step is to use (40) for the identification of the control parameters. Based on the previous Theorem, we can find the minimum permissible values for the control parameters $\boldsymbol{K}_\mathrm{p}, \boldsymbol{K}_\mathrm{d}$ and a_i. For $m = 1$, it is possible to find the parameters analytically, however, for $m \geq 2$, there is no analytical solution, but the parameters can be determined using numerical techniques for solving systems of non-linear equations, such as the Newton-Raphson method. We start with $m = 1$:

$$\dot{V} \leq -\frac{1}{2}\boldsymbol{x}^T\boldsymbol{Q}\boldsymbol{x} - \boldsymbol{x}^T\boldsymbol{SB}\boldsymbol{\phi} < 0.$$

To find an analytical solution for the parameters, the term $-(2a_{m-1} - \tilde{K})\boldsymbol{x}^T\boldsymbol{SBB}^T\boldsymbol{Sx}$ is ignored because $\dot{V} < 0$ if $a_{m-1} > \tilde{K}/2$. To satisfy the inequality, the following equations must hold:

$$\begin{aligned} \frac{1}{2}\boldsymbol{Q}|\boldsymbol{x}| &> \boldsymbol{SB}|\boldsymbol{\phi}_{\max}| \\ \frac{1}{2}\begin{bmatrix} \tilde{\boldsymbol{K}}\boldsymbol{K}_\mathrm{p}^2 & 0 & 0 \\ 0 & \tilde{\boldsymbol{K}}(\boldsymbol{K}_\mathrm{d}^2 - 2\boldsymbol{K}_\mathrm{p}) & 0 \\ 0 & 0 & \tilde{\boldsymbol{K}} \end{bmatrix}\boldsymbol{x} &> \begin{bmatrix} \boldsymbol{K}_\mathrm{p} \\ \boldsymbol{K}_\mathrm{d} \\ \boldsymbol{I} \end{bmatrix}|\boldsymbol{\phi}_{\max}|. \end{aligned} \quad (44)$$

Solving the above system of equations, we get

$$\begin{aligned} \tilde{\boldsymbol{K}}(i,i) &> \frac{2|\boldsymbol{\phi}_{\max}|}{\dot{\boldsymbol{e}}(i)}, \\ \boldsymbol{K}_\mathrm{p}(i,i) &> \frac{2|\boldsymbol{\phi}_{\max}|}{\tilde{\boldsymbol{K}}(i,i)\int \boldsymbol{e}(i)\,\mathrm{d}t}, \\ \boldsymbol{K}_\mathrm{d}(i,i) &> \sqrt{2\boldsymbol{K}_\mathrm{p}(i,i) + \left(\frac{|\boldsymbol{\phi}_{\max}|}{\tilde{\boldsymbol{K}}(i,i)\boldsymbol{e}(i)}\right)^2} - \frac{|\boldsymbol{\phi}_{\max}|}{\tilde{\boldsymbol{K}}(i,i)\boldsymbol{e}(i)}. \end{aligned}$$

Thus, for a given scenario, the control parameters can be easily identified by specifying the maximum acceptable $\boldsymbol{e}, \dot{\boldsymbol{e}}$ and $\int \boldsymbol{e}dt$. As mentioned earlier, $-(2a_{m-1} - \tilde{K})\boldsymbol{x}^T\boldsymbol{SBB}^T\boldsymbol{Sx}$ is ignored to find the control parameters. This term can be used to find the minimum values of parameters that will satisfy stability criteria for the system. However, there is no analytical solution in that case. The same procedure can be used to find the control parameters for $m \geq 2$. More about the parameters of the adaptive controller is presented in the next section.

B. DISCUSSION ON $\hat{\phi} \to \phi$

Another perspective of the proposed controller is to remove any mismatch during the system estimation. At any time t_o, the system dynamics can be written in Taylor series expansion form as

$$\boldsymbol{\phi}(t_o + h) = \boldsymbol{\phi}(t_o) + h\dot{\boldsymbol{\phi}}(t_o) + \frac{h}{2!}\ddot{\boldsymbol{\phi}}(t_o + h) + \cdots, \quad (45)$$

where $h > 0$. If h is assumed to be small such that

$$\boldsymbol{\phi}(t_o + h) \approx \boldsymbol{\phi}(t_o) + h\dot{\boldsymbol{\phi}}(t_o), \quad (46)$$

and we consider the case when the controller order $m = 2$, the control law (8) can be written as

$$\frac{\mathrm{d}^2\tilde{\boldsymbol{\phi}}(t_o)}{\mathrm{d}t^2} + a_1\frac{\mathrm{d}\tilde{\boldsymbol{\phi}}(t_o)}{\mathrm{d}t} + a_0\tilde{\boldsymbol{\phi}}(t_o) = \boldsymbol{0}. \quad (47)$$

From basic root-locus technique [43], the values for a_0 and a_1 can be chosen such that $\tilde{\boldsymbol{\phi}} \to \boldsymbol{0}$. A similar analogy can be used for the third-order controller, where the Taylor approximation will consider even the second-derivative of $\boldsymbol{\phi}$ and thus, the convergence will be faster. The condition (46) can be satisfied if the gains a_i are high enough to converge during the time h. We have shown the convergence of the estimated model towards the real model in the simulation results.

VI. COMPARISON WITH STATE-OF-THE-ART

We consider the following features to compare the proposed controller with the existing robust control methods: tuning the controller parameters, optimality, computational cost, robustness, dependence on model estimation, and practical implementation, especially for high DoF robotic manipulators. Another critical aspect of comparison is that most of the existing controllers do not have a performance analysis that can quantify the steady or transient-response behavior [5], [34].

Kim *et al.* [5] and Choi *et al.* [12] showed that a simple PID controller gives an optimal solution in terms of $\mathcal{H}_\infty$ optimality. Here, controller tuning requires knowledge about the parameters of the system. The proposed adaptive controller addresses all the above limitations discussed in this subsection. Apart from optimality, easy implementation and model-free control, there is a performance analysis that forces the steady-state error to be less than a prescribed value. More explanations are presented in the results. Table 1 summarizes all the controllers in a compact form.

VII. RESULTS

A 3-DoF and a 7-DoF robot manipulator (see Fig. 3) is considered to validate the proposed robust-adaptive controller. MATLAB Simulink with a sampling rate of 1 ms is used to implement the controller. The minimum allowed values for the controller are calculated using equation (44) and thus satisfy the performance criteria. In finding the control parameters, ignoring the term $-\boldsymbol{x}^T\boldsymbol{SBB}^T\boldsymbol{Sx}$ will still provide us with the optimal values. Although to find the absolute minimum

TABLE 1. Comparison:'-' means not completely true/known.

Approach	Reference(s)	Description	Quantitative performance	Easy tuning	Optimal	Model free
Lyapunov-based.	Slotine *et al.* [23]	Uses regressor matrix, advantage is guaranteed stability.	✖	✖	✖	✖
Lyapunov-based.	Kai *et al.* [2]	Uses linear orthogonal-basis functions to approximate the system dynamics. The advantage is that regressor matrix is replaced by simple basis functions.	✖	✖	✖	✓
Riccati inequality.	Bascetta *et al.* [25]	Uses regressor matrix. Advantage is that the PD gains of nominal system does not effect the robustness to uncertainties.	✖	-	✖	✖
Lyapunov-based two controllers.	Wang [29]	Uses regressor matrix. Address the kinematics and dynamics uncertainties.	-	✖	✖	✖
Regressor-based.	Pagilla *et al.* [28]	Uses observer to avoid joint velocity measurement.	✖	✖	✖	✖
Computed torque with modified outer-loop.	Peng *et al.* [26]	Deals with torque saturation and provides an improved and fast transient response. The controller requires system parameters for linearization.	-	✓	✖	✖
Lyapunov-based with an extra compensated term.	Na *et al.* [27]	Gives an improved transient response by adding a filtering term in the controller.	-	✖	✖	✖
Sliding-mode.	Yang *et al.* [30]	Uses a disturbance observer and a sliding-mode controller. Chattering is usually the major issue.	-	✖	✖	✓
Sliding-mode.	Yu *et al.* [22]	Switching control with average dwell-time. Disturbance observer is used for better robustness.	-	✓	✖	-
Finite-time.	Liu *et al.* [44]	Uses $\mathcal{H}_\infty$ approach to design the controller.	✓	✖	✓	✖
Orbital stability.	Pchelkin *et al.* [20]	Ensures that the real trajectory is always in a predefined orbit around the desired trajectory.	✓	✖	-	✖
PID controller using HJI equations.	Chung *et al.* [5], [12]	Introduces a performance limitation for the steady-state error using ISS. The control parameters require knowledge about system parameters.	✓	✖	✓	✓
Inverse optimal control using $\mathcal{H}_\infty$.	Proposed	-	✓	✓	✓	✓

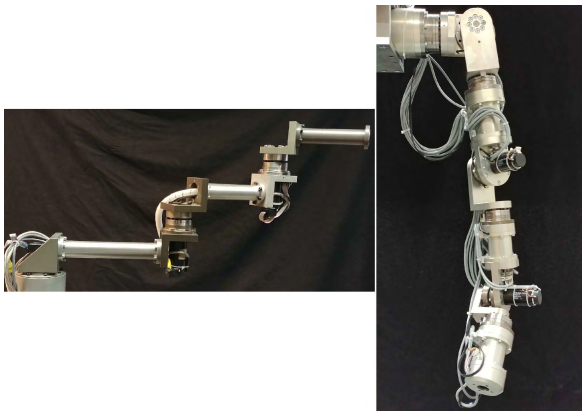

FIGURE 3. 3-DoF (left) and 7-DoF (right) robot manipulators used in experiments.

parameters, this term should be included and the Newton-Raphson method can be used to find the minimum values for acceptable control parameters. An easy and intuitive way to find the control parameters is to follow the steps mentioned below:

1) Find the minimum values for the control parameters using (40) that satisfy the condition for the maximum allowed joint-error at steady state.
2) Find the values of $\boldsymbol{K}_\mathrm{p}$ and $\boldsymbol{K}_\mathrm{d}$ using a performance criterion like rise-time, settling-time, etc.
3) Take a_i such that the gain of (47) is 3-5 times higher than (4).

The next two subsections present the simulation and experimental results for the 3-DoF manipulator. Because of the horizontal setup, the planar robot dynamics has no gravity term. Sec. VII-C discusses the effect of the order and gain of the controller. The results for the 7-DoF manipulator are shown in Sec. VII-D.

A. SIMULATION RESULTS

The desired trajectory for the end-effector of the manipulator is shown in Fig. 4. It was chosen heuristically and is in the workspace of the manipulator. The end-effector starts on the x-axis at 0.88 m from the base of the robot and it takes 6.17 s to complete one rotation. In this study, $m = 1$ and $m = 2$ is investigated. The threshold values for the state-errors are:

$$\boldsymbol{x}_{\max_1} = [10^{-3} \;\; 10^{-2} \;\; 10^{-1}]^T, \tag{48}$$

$$\boldsymbol{x}_{\max_2} = [10^{-4} \;\; 10^{-3} \;\; 10^{-2} \;\; 10^{-1}]^T, \tag{49}$$

where $\boldsymbol{x}_{\max_1}$ and $\boldsymbol{x}_{\max_2}$ are the maximum allowed errors in steady-state for $m = 1$ and $m = 2$, respectively.

The performance of the robot manipulator is shown in Fig. 5. The controller for $m = 2$ suffers from peaking and as a consequence, the trajectory of the end-effector shows a larger overshoot during the transient phase, see Fig. 5 and 6. Under the control parameters mentioned in table 1, the maximum permissible error after the transient response does not exceed (48) and (49), see Fig. 7. Because the selected values for the control parameters are higher than the required values

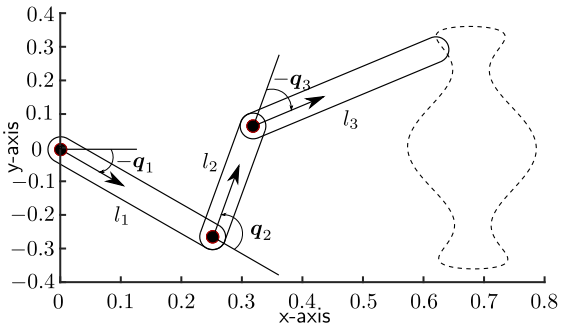

FIGURE 4. Top view of the 3-DoF robot manipulator along with the desired trajectory. The lengths are: $l_1 = 0.305$ *m*, $l_2 = 0.208$ *m* and $l_3 = 0.370$ *m*.

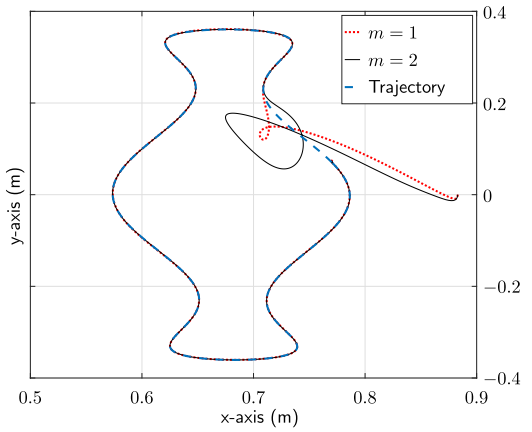

FIGURE 5. Simulation results: 3-DoF trajectory tracking in Cartesian space. The end-effector starts from (0.88 *m*,0 *m*) in the x-y coordinate system.

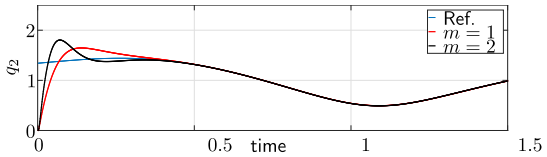

FIGURE 6. Trajectory for the second joint of the 3-DoF manipulator in simulation. Only the first 1.5 s are shown for clarity.

TABLE 2. Control parameters: (a) ignoring $-x^T SBB^T Sx$, (b) including $-x^T SBB^T Sx$, (c) Values used in controller.

Var.	$m = 1$			$m = 2$		
	(A)	(B)	(C)	(A)	(B)	(C)
$\tilde{K}$	222	3.3	68.9	174.7	63.4	68.9
K_p	200	78	400	57	100	400
K_d	32.3	0.0	40	39.9	20	40
b_0	-	-	-	0	20	69.6

for the specified performance, the maximum error $\boldsymbol{e}_{\max}$ is much smaller than the threshold value, which is 0.01 radians in our case ($\boldsymbol{x}_{\max_1}[2] = \boldsymbol{e}$ and $\boldsymbol{x}_{\max_2}[3] = \boldsymbol{e}$).

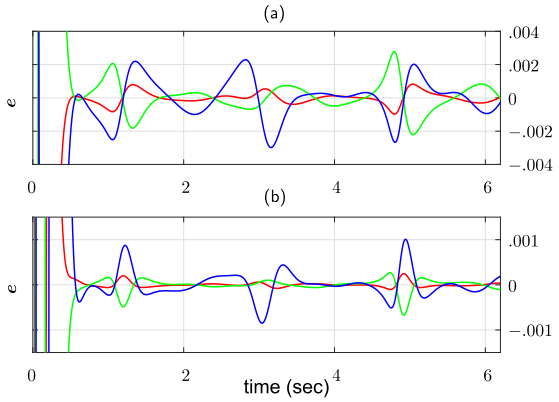

FIGURE 7. Satisfaction of performance criteria in simulation of 3-DoF robot. (a) $m = 1$. (b) $m = 2$. Red line: q_1, green line: q_2, blue line: q_3.

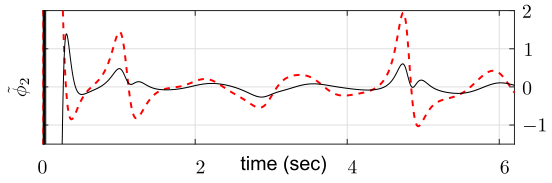

FIGURE 8. Difference between $\hat{\phi}$ and ϕ. Dashed line: $m = 1$, solid line: $m = 2$.

Fig. 8 shows the mismatch between the real and approximated model. Considering the same convergence rate for $m = 1$ and $m = 2$, the mismatch $\tilde{\boldsymbol{\phi}}$ is getting smaller as we increase the order of the controller. The obvious reason is that a higher order Taylor approximation gives better results, see Sec. V-B. However, the limitation of taking a higher order approximation is the peaking effect during the transient. One way of dealing with this problem is to start with $m = 1$ and as the mismatch approaches zero, we shift to a higher order approximation, because after the transient response, the torques for any order m are equal.

B. EXPERIMENTAL RESULTS

In simulations, we did not consider input saturation, disturbances and un-modeled parameters. Fortunately, they do not deteriorate the performance during the steady-state because these disturbances can be considered as part of $\boldsymbol{\phi}$, which is estimated by the controller during run-time. In experiments, the joint space result for the 3-DoF robot manipulator (Fig. 3) is shown in Fig. 9, and the trajectory tracking is shown in Fig. 10. The long transient-response is because of the torque-saturation; nevertheless, the performance criterion during steady-state is satisfied for both simulations and experiments. The errors in the joint angles are shown in Fig. 11, which satisfy the performance criteria (48) and (49). In the experiments, a comparison between real and approximated dynamics cannot be shown because we do not know the exact values of the actual system dynamics $\boldsymbol{\phi}$. As long as $\boldsymbol{\phi}$ is bounded, $\tilde{\boldsymbol{\phi}}$ will approach zero even in experiments.

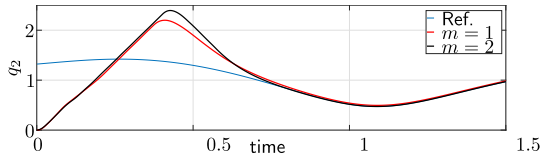

FIGURE 9. Trajectory for the second joint of the 3-DoF manipulator during experiment. Only the first 1.5 s are shown for clarity.

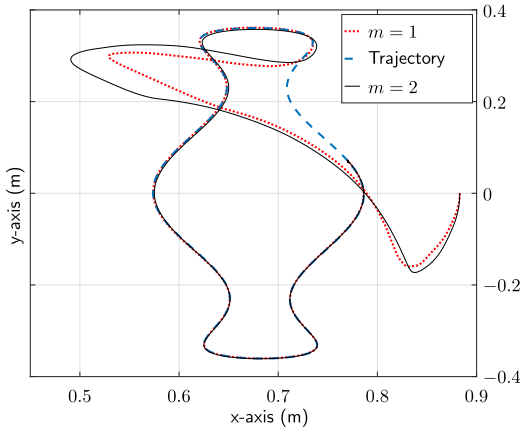

FIGURE 10. Experimental results: trajectory tracking in Cartesian space. Dashed line: $m = 1$, solid line: $m = 2$. The end-effector starts from (0.88 m,0) in the x-y coordinate system.

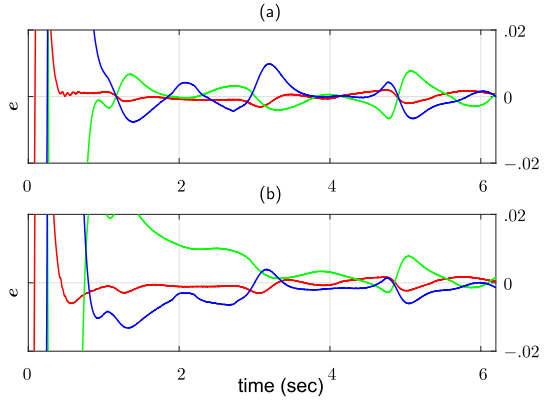

FIGURE 11. Experimental results for joint errors: (a) $m = 1$ (b) $m = 2$. Red line: q_1, green line: q_2, blue line: q_3. These figures shows that the control parameters satisfy the performance criteria of (48) and (49).

C. EFFECT OF ORDER AND GAIN OF CONTROLLER

For the proposed adaptive controller, the system dynamics $\boldsymbol{\phi}$ is approximated by a Taylor series of order $m-1$. Thus, for a first order approximation, the approximated system dynamics $\hat{\boldsymbol{\phi}}$ can only approach the true dynamics if $\boldsymbol{\phi}$ is constant. However, $\boldsymbol{\phi}$ depends on joint angles, velocities and acceleration, so unless the desired trajectory is slowly moving or the gain a_0 is high, there will always be a slight difference between $\hat{\boldsymbol{\phi}}$ and $\boldsymbol{\phi}$, as shown in Fig. 12.

By increasing the gain a_0, the estimated dynamics will converge faster, but more torque is required if the error is high. Also, if $\boldsymbol{\phi}$ is approaching a constant value, the estimated value

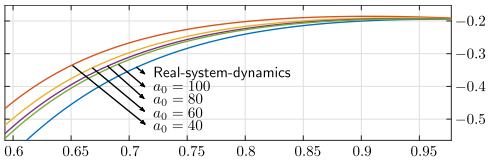

FIGURE 12. First order approximation with different a_0.

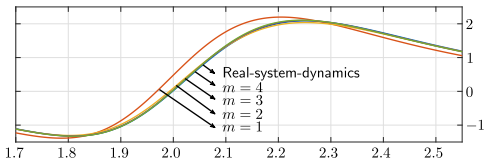

FIGURE 13. Various orders of control law with same convergence rate.

approaches the real system dynamics because the system acts like a Type 1 system [43]. However, if $\boldsymbol{\phi}$ is varying with time, the first order will never reach the real system dynamics as shown in Fig. 13.

To sum up, a first order approximation has no error for a constant $\boldsymbol{\phi}$, a second order has no error for a ramp $\boldsymbol{\phi}$, a third order approximation has no error for a hyperbolic $\boldsymbol{\phi}$ and so on. However, by selecting a sufficiently high gain a_i along with a second order approximation is quantitatively suitable to approximate the system dynamics. Fig. 13 shows the response of various orders for the same convergence rate.

The next point of interest is the effect of the order of the controller on the input torque. Once the error $\tilde{\boldsymbol{\phi}}$ approaches zero, then the torques will be equal for any order because the input torque is equal to

$$\boldsymbol{\tau}_{\text{in}} = \hat{\boldsymbol{\phi}} + \ddot{\boldsymbol{q}}_{\text{d}} - \boldsymbol{K}_{\text{d}}\dot{\boldsymbol{e}} - \boldsymbol{K}_{\text{p}}\boldsymbol{e}. \tag{50}$$

As long as $\hat{\boldsymbol{\phi}} \approx \boldsymbol{\phi}$, the torques for different m will remain equal.

D. EXPERIMENTAL RESULTS FOR 7-DoF ROBOT

The proposed adaptive controller is also used to control a 7-DoF manipulator, see Fig. 3. The motivation is to show that the performance criterion of (40) is satisfied for a 7 DoF robot. We performed experiments under the assumption that the system parameters are not known, and for that reason, we compared our proposed controller with a couple of model-free control methods. The performance in terms of the integral square error for the proposed controller is shown along with a simple PD and robust controller proposed by Choi *et al.* [12]. A more detailed comparison is given in [15]. The values of $\boldsymbol{K}_{\text{p}}$ and $\boldsymbol{K}_{\text{d}}$ are the same for the proposed and PD controllers for the experiment. For the robust controller [12], a trial and error method is chosen to tune the control parameters because of the assumption that the system parameters are not available. The integral square error

$$I(i) = \frac{1}{T_2 - T_1}\int_{T_1}^{T_2} e(i)^2 \mathrm{d}t, \quad i = 1, 2, .., 7 \tag{51}$$

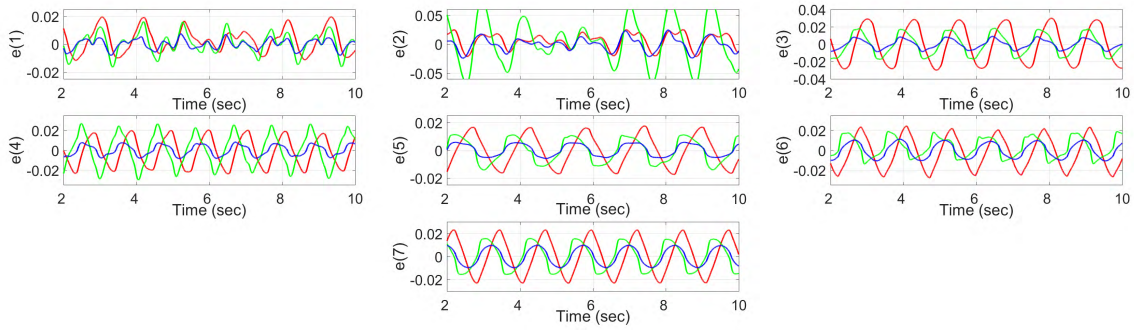

FIGURE 14. Errors in the joint angles: – PD controller, – robust controller [12] and – proposed controller.

TABLE 3. Error in the joint angles (rad).

joint	PD	Chung *et al.*	proposed
1	0.798×10^{-4}	0.537×10^{-4}	0.123×10^{-4}
2	1.910×10^{-4}	14.40×10^{-4}	1.240×10^{-4}
3	4.230×10^{-4}	1.440×10^{-4}	0.269×10^{-4}
4	2.050×10^{-4}	2.550×10^{-4}	0.276×10^{-4}
5	1.220×10^{-4}	0.731×10^{-4}	0.182×10^{-4}
6	2.660×10^{-4}	1.090×10^{-4}	0.548×10^{-4}
7	2.350×10^{-4}	1.260×10^{-4}	0.519×10^{-4}

for the three controllers are shown in table 3. Fig. 14 shows the error for each joint angle for sinusoidal references of different frequency and amplitude. During the steady-state, the integral square error for the proposed controller is much smaller compared to the other controllers. The order of the controller is $m = 1$, and the error reduction can be improved by taking higher order controller, however, the transient response will be worse. The gain of parameters of the adaptive controller can be reduced during the transient phase for improved response.

VIII. CONCLUSION AND FUTURE WORK

The main contribution of this paper is to implement an adaptive controller that satisfies a predefined performance with few tuning parameters required. For bounded disturbance, the controller is shown to be robust using the HJI equations. An inverse-optimal control method is utilized to evaluate an optimal cost function for the proposed controller. The control law is derived by using input-to-state-stability analysis that also ensures the stability of the system. The parameters of the proposed controller are identified using a quantitative performance analysis, which put an upper bound on the absolute values of the joint errors. The adaptive controller also ensures the removal of mismatch between real and estimated system model during feedback linearization to get better performance in terms of joint errors. Once the mismatch is removed, a PD controller can perform well to get the desired performance.

The proposed controller gives better results in terms of steady-state error by limiting the absolute error to a predefined maximum bound. However, there is no quantitative performance analysis for the transient phase and one way to improve the transient state is by using a funnel control.

REFERENCES

[1] C. Kim and K. Lee, "Robust control of robot manipulators using dynamic compensators under parametric uncertainty," *Int. J. Innov. Comput., Inf. Control*, vol. 7, no. 7, pp. 4129–4137, 2011.

[2] C. Y. Kai and A. C. Huang, "A regressor-free adaptive controller for robot manipulators without Slotine and Li's modification," *Robotica*, vol. 31, no. 7, pp. 1051–1058, 2013.

[3] M. C. Chien and A. C. Huang, "Adaptive impedance controller design for flexible-joint electrically-driven robots without computation of the regressor matrix," *Robotica*, vol. 30, no. 1, pp. 133–144, 2012.

[4] A. C. Huang, S. C. Wu, and W. F. Ting, "A FAT-based adaptive controller for robot manipulators without regressor matrix: Theory and experiments," *Robotica*, vol. 24, no. 2, pp. 205–210, 2006.

[5] M. J. Kim, Y. Choi, and W. K. Chung, "Bringing nonlinear $\mathcal{H}_\infty$ optimality to robot controllers," *IEEE Trans. Robot.*, vol. 31, no. 3, pp. 682–698, Jun. 2015.

[6] W. Khalil and E. Dombre, *Modeling, Identification and Control of Robots*. London, U.K.: Butterworth, 2004.

[7] M. W. Spong, S. Hutchinson, and M. Vidyasagar, *Robot Modeling and Control*, vol. 3. New York, NY, USA: Wiley, 2006.

[8] J. J. Craig, *Introduction to Robotics: Mechanics and Control*, vol. 3. Upper Saddle River, NJ, USA: Prentice-Hall, 2005.

[9] M. I. Ullah, S. A. Ajwad, R. U. Islam, U. Iqbal, and J. Iqbal, "Modeling and computed torque control of a 6 degree of freedom robotic arm," in *Proc. Int. Conf. Robot. Emerg. Allied Technol. Eng. (iCREATE)*, 2014, pp. 133–138.

[10] A. C. Bittencourt and S. Gunnarsson, "Static friction in a robot joint—Modeling and identification of load and temperature effects," *J. Dyn. Syst., Meas., Control*, vol. 134, no. 5, p. 051013, 2012.

[11] C. C. de Wit, H. Olsson, K. J. Astrom, and P. Lischinsky, "A new model for control of systems with friction," *IEEE Trans. Autom. Control*, vol. 40, no. 3, pp. 419–425, Mar. 1995.

[12] Y. Choi, W. K. Chung, and I. H. Suh, "Performance and $\mathcal{H}_\infty$ optimality of PID trajectory tracking controller for Lagrangian systems," *IEEE Trans. Robot. Autom.*, vol. 17, no. 6, pp. 857–869, Dec. 2001.

[13] J. Park and W. K. Chung, "Analytic nonlinear $\mathcal{H}_\infty$ inverse-optimal control for Euler-Lagrange system," *IEEE Trans. Robot. Autom.*, vol. 16, no. 6, pp. 847–854, Dec. 2000.

[14] A. Del Prete and N. Mansard, "Robustness to joint-torque-tracking errors in task-space inverse dynamics," *IEEE Trans. Robot.*, vol. 32, no. 5, pp. 1091–1105, Oct. 2016.

[15] R. Hayat and M. Buss, "Model identification for robot manipulators using regressor-free adaptive control," in *Proc. UKACC 11th Int. Conf. Control (UKACC)*, 2016, pp. 1–7.

[16] L. Yu, S. Fei, L. Sun, J. Huang, and G. Yang, "Design of robust adaptive neural switching controller for robotic manipulators with uncertainty and disturbances," *J. Intell. Robotic Syst.*, vol. 77, nos. 3–4, pp. 571–581, 2015.

[17] L. Yu and S. Fei, "Robustly stable switching neural control of robotic manipulators using average dwell-time approach," *Trans. Inst. Meas. Control*, vol. 36, no. 6, pp. 789–796, 2014.

[18] B. Xiao, S. Yin, O. Kaynak, and H. Gao, "Observer-based control for robotic manipulations with uncertain kinematics and dynamics," in *Proc. IEEE 14th Int. Workshop Adv. Motion Control (AMC)*, Apr. 2016, pp. 282–288.

[19] J. Qin, F. Léonard, and G. Abba, "Real-time trajectory compensation in robotic friction stir welding using state estimators," *IEEE Trans. Control Syst. Technol.*, vol. 24, no. 6, pp. 2207–2214, Nov. 2016.

[20] S. S. Pchelkin *et al.*, "On orbital stabilization for industrial manipulators: Case study in evaluating performances of modified PD+ and inverse dynamics controllers," *IEEE Trans. Control Syst. Technol.*, vol. 25, no. 1, pp. 101–117, Jan. 2017.

[21] A. Ferrara and G. P. Incremona, "Design of an integral suboptimal second-order sliding mode controller for the robust motion control of robot manipulators," *IEEE Trans. Control Syst. Technol.*, vol. 23, no. 6, pp. 2316–2325, Nov. 2015.

[22] L. Yu, J. Huang, and S. Fei, "Sliding mode switching control of manipulators based on disturbance observer," *Circuits, Syst., Signal Process.*, vol. 36, no. 6, pp. 2574–2585, 2017.

[23] J.-J. E. Slotine and W. Li, "On the adaptive control of robot manipulators," *Int. J. Robot. Res.*, vol. 6, no. 3, pp. 49–59, 1987.

[24] B. Siciliano, L. Sciavicco, L. Villani, and G. Oriolo, *Robotics: Modelling, Planning and Control*. London, U.K.: Springer-Verlag, 2009. [Online]. Available: https://www.springer.com/de/book/9781846286414

[25] L. Bascetta and P. Rocco, "Revising the robust-control design for rigid robot manipulators," *IEEE Trans. Robot.*, vol. 26, no. 1, pp. 180–187, Feb. 2010.

[26] W. Peng, Z. Lin, and J. Su, "Computed torque control-based composite nonlinear feedback controller for robot manipulators with bounded torques," *IET Control Theory Appl.*, vol. 3, no. 6, pp. 701–711, Jun. 2009.

[27] J. Na, G. Herrmann, and K. Zhang, "Improving transient performance of adaptive control via a modified reference model and novel adaptation," *Int. J. Robust Nonlinear Control*, vol. 27, no. 8, pp. 1351–1372, 2017.

[28] R. P. Pagilla and M. Tomizuka, "An adaptive output feedback controller for robot arms: Stability and experiments," *Automatica*, vol. 37, no. 7, pp. 983–995, 2001.

[29] H. Wang, "Adaptive control of robot manipulators with uncertain kinematics and dynamics," *IEEE Trans. Autom. Control*, vol. 62, no. 2, pp. 948–954, Feb. 2017.

[30] Z.-J. Yang, Y. Fukushima, and P. Qin, "Decentralized adaptive robust control of robot manipulators using disturbance observers," *IEEE Trans. Control Syst. Technol.*, vol. 20, no. 5, pp. 1357–1365, Sep. 2012.

[31] C. Zhang and H.-S. Yan, "Inverse control of multi-dimensional taylor network for permanent magnet synchronous motor," *Int. J. Comput. Math. Electr. Electron. Eng.*, vol. 36, no. 6, pp. 1676–1689, 2017.

[32] M. M. Fateh, S. Azargoshasb, and S. Khorashadizadeh, "Model-free discrete control for robot manipulators using a fuzzy estimator," *Int. J. Comput. Math. Electr. Electron. Eng.*, vol. 33, no. 3, pp. 1051–1067, 2014.

[33] A. Safaei, Y. C. Koo, and M. N. Mahyuddin, "Adaptive model-free control for robotic manipulators," in *Proc. IEEE Int. Symp. Robot. Intell. Sensors (IRIS)*, Oct. 2017, pp. 7–12.

[34] H. G. Sage, M. F. De Mathelin, and E. Ostertag, "Robust control of robot manipulators: A survey," *Int. J. Control*, vol. 72, no. 16, pp. 1498–1522, 1999.

[35] C. P. Bechlioulis, M. V. Liarokapis, and K. J. Kyriakopoulos, "Robust model free control of robotic manipulators with prescribed transient and steady state performance," in *Proc. RSJ Int. Conf. Intell. Robots Syst. (IROS)*, 2014, pp. 41–46.

[36] M. Krstic and Z.-H. Li, "Inverse optimal design of input-to-state stabilizing nonlinear controllers," *IEEE Trans. Autom. Control*, vol. 43, no. 3, pp. 336–350, Mar. 1998.

[37] B. S. Chen, T. S. Lee, and J. H. Feng, "A nonlinear $\mathcal{H}_\infty$ control design in robotic systems under parameter perturbation and external disturbance," *Int. J. Control*, vol. 59, no. 2, pp. 439–461, 1994.

[38] H. K. Khalil, *Noninear Systems*. Upper Saddle River, NJ, USA: Prentice-Hall, 1996.

[39] F. L. Lewis, D. Vrabie, and V. L. Syrmos, *Optimal Control*, vol. 3. Hoboken, NJ, USA: Wiley, 2012.

[40] E. D. Sontag and Y. Wang, "On characterizations of the input-to-state stability property," *Syst. Control Lett.*, vol. 24, no. 5, pp. 351–359, 1995.

[41] E. D. Sontag, "Smooth stabilization implies coprime factorization," *IEEE Trans. Autom. Control*, vol. 34, no. 4, pp. 435–443, Apr. 1989.

[42] E. D. Sontag, "Input to state stability: Basic concepts and results," in *Nonlinear and Optimal Control Theory*. Berlin, Gemany: Springer-Verlag, 2008, pp. 163–220. [Online]. Available: https://link.springer.com/chapter/10.1007/978-3-540-77653-6_3

[43] K. Ogata, *Modern Control Engineering*, 5th ed. Upper Saddle River, NJ, USA: Prentice-Hall, 2009, p. 55.

[44] H. Liu, X. Tian, G. Wang, and T. Zhang, "Finite-time $\mathcal{H}_\infty$ control for high-precision tracking in robotic manipulators using backstepping control," *IEEE Trans. Ind. Electron.*, vol. 63, no. 9, pp. 5501–5513, Sep. 2016.

[45] S. R. Munasinghe, M. Nakamura, S. Aoki, S. Goto, and N. Kyura, "High speed precise control of robot arms with assigned speed under torque constraint by trajectory generation in joint co-ordinates," in *Proc. IEEE Int. Conf. Syst., Man, Cybern.*, vol. 2, Oct. 1999, pp. 854–859.

[46] V. Mhase, R. Sudarshan, O. Pardeshi, and P. V. Suryawanshi, "Integrated speed–position tracking with trajectory generation and synchronization for 2–axis DC motion control," *Int. J. Eng. Res. Develop.*, vol. 1, no. 6, pp. 61–66, 2012.

[47] S. H. Chong and K. Sato, "Practical and robust control for precision positioning systems," in *Proc. IEEE Int. Conf. Mechatronics (ICM)*, Apr. 2011, pp. 961–966.

[48] C. D. Sousa and R. Cortesão, "Physical feasibility of robot base inertial parameter identification: A linear matrix inequality approach," *Int. J. Robot. Res.*, vol. 33, no. 6, pp. 931–944, 2014.

[49] J. Swevers, C. Ganseman, D. B. Tükel, J. de Schutter, and H. Van Brussel, "Optimal robot excitation and identification," *IEEE Trans. Robot. Autom.*, vol. 13, no. 5, pp. 730–740, Oct. 1997.

[50] T. Basar and G. J. Olsder, *Dynamic Noncooperative Game Theory*, vol. 23. Philadelphia, PA, USA: SIAM, 1999.

[51] A. J. van der Schaft, "L_2-gain analysis of nonlinear systems and nonlinear state-feedback H_∞ control," *IEEE Trans. Autom. Control*, vol. 37, no. 6, pp. 770–784, Jun. 1992.

[52] S. Yin, X. Li, H. Gao, and O. Kaynak, "Data-based techniques focused on modern industry: An overview," *IEEE Trans. Ind. Electron.*, vol. 62, no. 1, pp. 657–667, Jan. 2015.

[53] M. Jin, S. H. Kang, P. H. Chang, and J. Lee, "Robust control of robot manipulators using inclusive and enhanced time delay control," *IEEE/ASME Trans. Mechatronics*, vol. 22, no. 5, pp. 2141–2152, Oct. 2017.

RAMEEZ HAYAT received the M.S. degree in electronic engineering from the Ghulam Ishaq Khan Institute of Engineering Sciences and Technology, Pakistan, in 2012. He is currently pursuing the Ph.D. degree with the Technical University of Munich, Germany. He is a Research Associate with the Chair of Automatic Control Engineering, Technical University of Munich. His research interests include adaptive control, optimal control, system identification, and control of under-actuated systems.

MARION LEIBOLD received the Diploma degree in applied mathematics and the Ph.D. degree in electrical engineering from the Technical University of Munich, Germany, in 2002 and 2007, respectively. She is currently a Lecturer with the Chair of Automatic Control Engineering, Technical University of Munich. Her research interests include hybrid dynamical systems, optimal control, and legged robots.

MARTIN BUSS received the Diploma Engineering degree in electrical engineering from the Technical University of Darmstadt, Darmstadt, Germany, in 1990, the D. Eng. degree in electrical engineering from the University of Tokyo, Tokyo, Japan, in 1994, and the Habilitation degree from the Technical University of Munich, Munich, Germany, in 2000. In 1988, he was a Research Student for one year with the Science University of Tokyo. From 1994 to 1995, he was a Post-Doctoral Researcher with the Department of Systems Engineering, Australian National University, Canberra, Australia. From 1995 to 2000, he was a Senior Research Assistant and a Lecturer with the Chair of Automatic Control Engineering, Department of Electrical Engineering and Information Technology, Technical University of Munich. From 2000 to 2003, he was a Full Professor, the Head of the Control Systems Group, and the Deputy Director of the Institute of Energy and Automation Technology, Faculty IV, Electrical Engineering and Computer Science, Technical University of Berlin, Berlin, Germany. Since 2003, he has been a Full Professor (Chair) with the Chair of Automatic Control Engineering, Faculty of Electrical Engineering and Information Technology, Technical University of Munich, where he has been with the Medical Faculty since 2008. Since 2006, he has also been the Coordinator of the Deutsche Forschungsgemeinschaft Excellence Research Cluster Cognition for Technical Systems with CoTeSys. His research interests include automatic control, mechatronics, multimodal human system interfaces, optimization, and non-linear and hybrid discrete-continuous systems.